Available online at www.sciencedirect.com
SCIENCE DIRECT®
Vision Research 44 (2004) 1879–1889
Vision Research
www.elsevier.com/locate/visres

Path perception during rotation: influence of instructions, depth range, and dot density

Li Li *, William H. Warren Jr.

Department of Cognitive and Linguistic Sciences, Brown University, Box 1978, Providence, RI 02912, USA

Received 1 October 2003; received in revised form 5 March 2004

Abstract

How do observers perceive their direction of self-motion when traveling on a straight path while their eyes are rotating? Our previous findings suggest that information from retinal flow and extra-retinal information about eye movements are each sufficient to solve this problem for both perception and active control of self-motion [Vision Res. 40 (2000) 3873; Psych. Sci. 13 (2002) 485]. In this paper, using displays depicting translation with simulated eye rotation, we investigated how task variables such as instructions, depth range, and dot density influenced the visual system's reliance on retinal vs. extra-retinal information for path perception during rotation. We found that path errors were small when observers expected to travel on a straight path or with neutral instructions, but errors increased markedly when observers expected to travel on a curved path. Increasing depth range or dot density did not improve path judgments. We conclude that the expectation of the shape of an upcoming path can influence the interpretation of the ambiguous retinal flow. A large depth range and dense motion parallax are not essential for accurate path perception during rotation, but reference objects and a large field of view appear to improve path judgments.

Keywords: Eye movement; Heading; Optic flow; Self-motion

1. Introduction

Accurate perception of the direction of self-motion, or *heading*, appears to be important for successful locomotion in the world (Gibson, 1950; Warren, Kay, Zosh, Duchon, & Sahuc, 2001). Previous studies have shown that when traveling on a straight path with no eye, head or body rotation, people can accurately judge their heading from the radial pattern of optic flow, which contains a focus of expansion (FOE) in the heading direction (Warren, 2004; Warren, Morris, & Kalish, 1988). This is even the case for visually impaired patients with a field of view as narrow as 5° (Li, Peli, & Warren, 2002). However, the perception of heading becomes more complicated when the observer is rotating his/her eye while traveling on a straight path. The eye rotation adds a rotational component to the flow, which alters the radial pattern, eliminates the FOE in the observer's heading direction, and creates a spurious focus at the fixation point if it is attached to the environment. Formal analyses have shown that the instantaneous retinal velocity field in this case is equivalent to the field created by traveling on a curved path with no eye rotation (Royden, 1994).

In this article we pursue the question of how people recover heading and perceive their *path* of self-motion during eye rotation. Some previous psychophysical results support the view that heading can be recovered from the retinal flow alone because the components due to translation and rotation have different properties (Cutting, Springer, Braren, & Johnson, 1992; Stone & Perrone, 1997; van den Berg, 1992; van den Berg & Brenner, 1994a, 1994b; Wang & Cutting, 1999; Warren & Hannon, 1988, 1990). Specifically, *motion parallax* between elements at different depths corresponds to observer translation (Rieger & Lawton, 1985), whereas common *lamellar motion* across the visual field corresponds to observer rotation (Koenderink & van Doorn, 1987; Perrone, 1992). However, other results support the view that extra-retinal information about eye movements is necessary to compensate for the rotation,

* Corresponding author. Address: NASA Ames Research Center, MS 262-2, Moffett Field CA 94035, USA. Tel.: +1-650-604-5905; fax: +1-650-604-0255.
E-mail address: lli@mail.arc.nasa.gov (L. Li).

0042-6989/$ - see front matter © 2004 Elsevier Ltd. All rights reserved.
doi:10.1016/j.visres.2004.03.008

especially at high rotation rates (>1°/s) (Banks, Ehrlich, Backus, & Crowell, 1996; Ehrlich, Beck, Crowell, Freeman, & Banks, 1998; Royden, Banks, & Crowell, 1992; Royden, Crowell, & Banks, 1994).

One drawback to these studies is that they used random-dot displays, which place inherent restrictions on dot density and depth range, and do not contain environmental objects. Restricted dot density and depth range both limit the motion parallax available in the display, and the restricted depth range also limits static depth information that could be used to help estimate the rotation (van den Berg & Brenner, 1994b). We recently found that observers are more accurate in both judging and actively controlling their path of self-motion with dense texture-mapped displays that include reference objects (Li & Warren, 2000, 2002; see also Cutting, Vishton, Fluckiger, Baumberger, & Gerndt, 1997). We proposed that the visual system recovers the instantaneous heading in the *retinal coordinate system* on the basis of dense motion parallax, and recovers the path in the *world coordinate system* by updating heading with respect to reference objects in the scene. This is consistent with previous analyses showing that, while information in a single velocity field specifies the instantaneous retino-centric heading unambiguously, information must be integrated over time to distinguish various possible paths in the world (Stone & Perrone, 1997; Warren, Blackwell, Kurtz, Hatsopolous, & Kalish, 1991). We thus demonstrated that retinal flow alone is sufficient for path perception during rotation; extra-retinal information also contributes but is not necessary (see also Crowell & Andersen, 2001; Grigo & Lappe, 1999).

It is important to recognize that there is a cue conflict between retinal and extra-retinal information under simulated rotation conditions. As noted above, the instantaneous retinal flow field for traveling on a straight path with eye rotation is equivalent to that for traveling on a curved path with no eye rotation, with the curvature of the path defined by the ratio between the instantaneous translation and the eye rotation rate (Royden, 1994). In displays with simulated rotation, the flow pattern on the screen depicts the effect of forward translation plus an eye rotation, but the eye actually remains stationary. Thus, any extra-retinal signals would indicate zero eye rotation. If the visual system relies on extra-retinal signals, the rotational component in the flow will be attributed to a curved path in the world. On the other hand, the retinal flow specifies that the heading is fixed in the visual environment, but if one were traveling on a curved path, the heading should shift with respect to objects over time. Thus, if the visual system relies on retinal information, the rotational component in the flow will be attributed to observer rotation and travel on a straight path will be perceived. Such a conflict may account for the many inconsistent results in the heading perception literature. If so, we should be able to push the observer toward a straight or curved path percept by manipulating the information and the task.

We previously showed that, with texture-mapped displays that contain dense parallax and reference objects, observers can judge their path with an accuracy of a few degrees despite conflicting extra-retinal signals (Li & Warren, 2000). In the present experiments, we investigated how task variables such as instructions influenced observers' path judgments. Specifically, using displays with simulated eye rotation, we told observers that they were traveling on a straight path (consistent with retinal information), a curved path (consistent with extra-retinal information), or did not mention the shape of the path. In addition, we examined whether varying the depth range and dot density in random-dot displays influenced path performance. The depth range and dot density affect static depth and motion parallax information available in the display. We found that for both texture-mapped and random-dot displays, path errors were small when observers were not informed of the shape of the path. Observers given straight and curved path instructions had large differences in performance and actually thought they were viewing two different classes of displays. Increasing the depth range in random-dot displays reduced path errors only with curved path instructions, and there were no effects of dot density. The results lead us to propose that, under cue conflict conditions such as translation with simulated eye rotation, the expectation that one is on a straight or curved path can push the visual system toward a straighter or more curved interpretation of the ambiguous retinal flow. Static depth or dense motion parallax may not be the essential sources of retinal information for accurate path perception during rotation.

2. General method

2.1. Displays

The displays, which were similar to those of Li and Warren (2000), depicted the flow pattern for an observer traveling over a ground plane on a straight path at a fast walking speed of 2 m/s with an eye height of 1.6 m, while fixating to one side. The path direction was varied along a horizontal axis and the observer's task was to position a probe on the perceived future path at the end of each 1.5 s trial. The fixation point was a red circle at eye level, on top of a post that was attached to the ground plane. In the *actual rotation condition* (which depicted real-world tracking under this situation), a radial flow pattern was presented on the screen. The fixation point moved horizontally on the screen, its angular velocity gradually increasing as the observer traveled forward, and observers tracked its motion with a pursuit eye movement. The flow pattern on the observer's retina was thus produced by the sum of a translation and a real eye rotation. In the *simulated rotation condition*, the flow pattern on the screen simulated the sum of a translation and a rotation (with a gradually increasing angular velocity), but the fixation point remained stationary on the screen so no actual eye movement occurred. The flow pattern on the retina was the same in both conditions, whereas extra-retinal information was manipulated: it was consistent with the rotational component of flow in the first case, but inconsistent in the second case because any extra-retinal signal specified zero rotation. With a fixation point attached to the environment, the rate of eye rotation necessarily increases as the observer moves forward, so following previous practice we specified the mean rotation rate (0, ±3, or ±5°/s) for a 1.5 s trial. Mean rotation rate is determined by the average of the instantaneous rotation rate over the duration of a trial. Positive values are to the right of center screen, negative values to the left. Final fixation angles were chosen for each mean rotation rate so that the final angle did not co-vary with the mean rotation rate. This resulted in the fixation point distance varying from 6 to 13 m from trial to trial (see details in Li & Warren, 2000).

A trial was created in the following way. The nominal Z axis of the simulated environment was initially perpendicular to the center of the screen. The path direction was randomly chosen within ±10° about this Z axis. Next the fixation post was positioned on the ground plane at an initial β up to 19.5° (final β up to 30°) from the path direction, so that it would produce a specified mean rotation rate for the trial. In the actual condition, the path remained in its original screen location while the fixation point moved, generating the effects of an actual pursuit eye movement. In the simulated condition, the "camera" at the eye point was turned about a vertical axis so that the fixation point appeared in a random position within ±10° of the center of the screen at the start of a trial, so the path appeared at an initial angle up to ±29.5° (final angle up to ±40°) from the center of the screen. This was done to limit the fixation point's initial eccentricity and keep both it and the path point on screen throughout the trial. The "camera" then rotated during the trial to keep the fixation point stationary on the screen, simulating the effects of a pursuit eye movement.

The displays were generated on a Silicon Graphics Crimson Reality Engine at a frame rate of 30 Hz, and were rear-projected on a large screen (112° H × 95° V) with a Barco 800 graphics projector with a 60 Hz refresh rate. Observers viewed the screen monocularly from a chin rest using their preferred eye. The chin rest was placed at a distance of 1 m, positioned at the display's center of projection at a height of 1.6 m. The edges of the screen were in the periphery against a black background in a dark room, minimizing the possibility that they might provide a stationary frame of reference.

2.2. Procedure

On each trial, the first frame appeared for 1 s to allow observers to fixate the fixation point, followed by 1.5 s of motion. The motion then stopped, the last frame remained visible, and a blue probe line (9.1° tall) appeared on the ground at a distance of 10 m. The azimuth position of the probe could be adjusted along an arc with a 10 m radius using the mouse. Observers were instructed to track the fixation point throughout the trial and, at the end of the trial, to position the probe on their perceived future path, assuming they continued to travel on their present path. The probe and the last frame remained visible until they clicked a mouse button, which started the next trial. To make sure observers understood the task and the response device, they received a set of practice trials before each condition. No feedback was provided on any trial. An experimental session typically lasted less than an hour.

3. Experiment 1

The purpose of the first experiment was to investigate whether instructions about the shape of the path can bias the observer's interpretation of the ambiguous velocity field during simulated rotation. We used three sets of instructions: observers were told they were traveling on a *straight* path, a *curved* path, or else the shape of the path was not mentioned (*neutral*). Two display conditions were tested: the *textured ground* (Fig. 1a) provided a dense motion parallax across the ground plane and one reference object (the fixation post), whereas *dense posts* (Fig. 1b) contained motion parallax among objects, and multiple reference objects. We previously found that both of these displays allowed accurate path judgments under simulated rotation with neutral instructions, despite conflicting extra-retinal signals (Li & Warren, 2000).

The straight path instructions are consistent with the retinal information for translation with simulated eye rotation, so if they bias the visual system to rely on retinal information about the current path, we would expect small errors. Conversely, the curved path instructions are consistent with extra-retinal signals for zero eye rotation. Hence, if they bias the visual system to rely on extra-retinal information, we would expect observers to perceive curved paths of self-motion, and thus the path error should increase markedly with rotation rate.

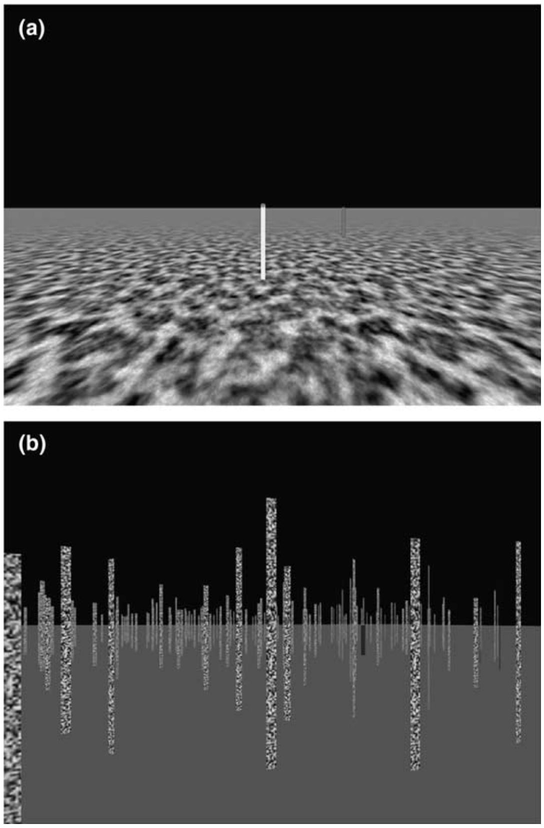

Fig. 1. A sample last frame in each display condition in Experiment 1. The fixation post is in the center and the probe (gray) to indicate the future path is on the right: (a) textured ground and (b) dense posts.

3.1. Method

Participants. Ten students and staff at Brown University were paid to participate, all with normal or corrected-to-normal vision. Among them, four were experienced subjects and the rest were participating in a path perception experiment for the first time. We observed no systematic performance differences between the experienced and the naïve observers.

Displays. We tested mean eye rotation rates of 0, ±3, and ±5°/s in the simulated rotation condition. As a control, we tested mean rotation rates of ±5°/s in the actual rotation condition. The mean rotation rates were crossed with two display conditions. (1) *Textured ground* (Fig. 1a): The ground plane (240 m wide × 120 m deep) was texture-mapped and the sky was black. The texture map was composed of a filtered noise pattern with a power spectrum of $1/f^2$ for the range of frequencies from 8 to 32 cycles across the image. The image was anti-aliased with a mipmap-bilinear minification filter. A red fixation point appeared at the top of a white post that was anchored to the ground, providing a reference object in the display. (2) *Dense posts* (Fig. 1b): The ground plane was a flat green (240 m wide × 120 m deep), with 231 granite-textured posts positioned in 7 rows of 33 posts each, spanning a depth range of 1–18 m. The distance of posts between rows varied randomly from 1.5 to 4.5 m, and the distance between posts within a row varied randomly from 0.4 to 1.2 m, with a density of about 0.5 posts/m^2. Each post was 0.11 m wide, varied randomly in height between 2–3 m, and was randomly rotated out of the frontal plane from −35° to +35° about its vertical axis. A red fixation point was attached to one of the posts.

Instructions. Three sets of instructions were tested. (1) *Straight path*: Observers were told that the display depicted their walking on a straight path while looking at an object off to one side. (2) *Curved path*: Observers were told that the display simulated their walking on a curved path while looking at an object off to one side. (3) *Neutral*: Observers were told that the display depicted their traveling on a path while looking at an object off to one side. The shape of the path was not mentioned.

Procedure. Trials were presented in two test sessions, one for each display type. In each session, the three sets of instructions and the actual rotation condition were tested in a random order, with 10 practice trials before each set of instructions. In the actual rotation condition, only the neutral instructions were tested. Subjects participated in both test sessions in a counterbalanced order, about one day apart. There were 105 trials (21 trials for each eye rotation rate) in each path instructions condition and 42 trials in the actual rotation condition, for a total of 377 trials in a session. Trials were blocked by testing condition and randomized within blocks.

3.2. Results

Mean constant path error for the textured ground display is plotted as a function of mean rotation rate in Fig. 2a. A flat function indicates that path judgments are unaffected by rotation rate, whereas a positive slope indicates that error increases in the direction of rotation, and a negative slope that error increases in the opposite direction. The data for the curved path instructions show large errors in the direction of rotation, up to 12° at 5°/s. This is consistent with the perception of a curved path of self-motion, which observers reported in a debriefing, and the magnitude of the effect is comparable to that of Royden et al. (1992, 1994) for random-dot displays with neutral instructions.

On the other hand, path errors are significantly smaller in the other path instructions conditions, remaining below 7° with the neutral instructions, and below 4° with the straight path instructions, across all rotation rates. A multivariate regression analysis reveals that slope in the neutral instructions condition (1.29) is reliably shallower than that in the curved path instructions condition (2.19), $t(162) = 3.16$, $p < 0.01$. There are indications that the straight path instructions may reduce errors further, for the slope (0.76) is marginally

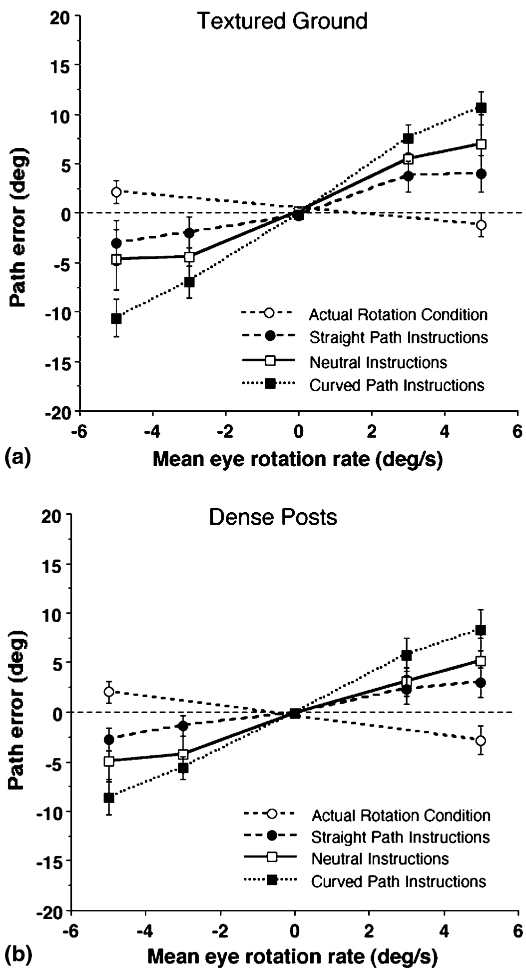

Fig. 2. Mean path error as a function of rotation rate in Experiment 1: (a) textured ground and (b) dense posts. Error bars represent between-subjects SEs.

shallower than that for neutral instructions, $t(162) = 1.87$, $p = 0.062$. However, the straight slope is still greater than that in that actual rotation condition (−0.33), $t(162) = 3.52$, $p < 0.001$, which is not significantly different from 0, $t(36) = -1.99$, *ns*, and is thus statistically flat. This confirms the contribution of extra-retinal information in path recovery during rotation. The slopes for both the straight path and the neutral instructions are statistically greater than 0, with $t(96) = 4.8$, $p < 0.0001$ and $t(96) = 5.67$, $p < 0.0001$, respectively.

A similar pattern of results is found for the dense posts display (Fig. 2b). The slope in the curved path instructions condition (1.74) is significantly greater that that in the neutral instructions condition (1.06), $t(162) = 2.92$, $p < 0.01$, where mean errors remain below 5° at all rotation rates. The straight path instructions reduce mean errors to below 3°, with a slope (0.58) that is significantly shallower than that for the neutral instructions, $t(162) = 2.09$, $p < 0.05$. In this case, the slope in the actual rotation condition is negative (−0.49) and significantly different from 0, $t(162) = -2.55$, $p < 0.05$, indicating that some observers may be overestimating the visual angle between the path direction and the fixation direction by a couple of degrees. If this were also true for the simulated rotation, it would artificially reduce the estimated path errors overall, but would not affect the differences between path instructions conditions. Multivariate regression analyses indicate that although the slopes for the dense posts display are shallower than those for the textured ground display, they are not statistically different: for the curved path instructions, $t(96) = -1.88$, *ns*, for the neutral instructions, $t(96) = -0.71$, *ns*, and for the straight path instructions, $t(96) = -0.80$, *ns*.

In a debriefing immediately following the test session, eight out of ten subjects (including two experienced subjects) reported seeing two different classes of displays for the straight and the curved path instructions.

3.3. Discussion

First, the results demonstrate that straight or curved path instructions can influence observers' interpretation of the retinal flow under cue conflict conditions. For both the textured ground and the dense posts displays, the curved path instructions significantly increased path errors, whereas the straight path instructions significantly improved accuracy. The fact that observers reported seeing different classes of displays in the different path instructions conditions indicates that this was not merely a response bias, but reflected their perceptual experience of the displays. We suggest that the instructions may have led observers to resolve the path ambiguity by differentially relying on retinal information (such as dense motion parallax and reference objects) that was consistent with a straight path, or on extra-retinal signals for zero eye rotation that were consistent with a curved path.

Second, the results confirm previous findings that both retinal and extra-retinal information contribute to recovering the path of self-motion during rotation. With neutral instructions, mean path errors remain below 7° for the ground plane and below 5° for the dense posts during simulated rotation, compared with previous errors of 15° at 5°/s for random-dot displays (Ehrlich et al., 1998; Li & Warren, 2000; Royden et al., 1992, 1994). This replicates our finding that given sufficient retinal information, the visual system depends primarily on retinal flow and can determine the path of self-motion to within a few degrees, even with conflicting extra-retinal signals (Li & Warren, 2000, 2002). Such a pattern of results demonstrates that extra-retinal information is not necessary to recover the path of self-motion with reasonable accuracy. However, more accurate judgments were obtained in the actual rotation condition, when extra-retinal signals about eye position were concordant with the retinal information. This result confirms earlier findings that extra-retinal signals can contribute to path perception during eye rotation.

4. Experiment 2

The previous experiment examined the effect of instructions on the perceived path of self-motion using texture-mapped displays that contained dense motion parallax, a large depth range, and reference objects. In the present experiment, we tested whether instructions similarly help to resolve the path ambiguity in random-dot displays, where observers tend to see a highly curved path of self-motion (Banks et al., 1996; Li & Warren, 2000; Royden, 1994). In addition, we manipulated the visible depth range and the dot density of the ground plane to determine whether these variables influence the perceived path in random-dot displays. As noted before, the depth range and dot density affect the static depth and motion parallax information available in the display.

We used again the straight path, the curved path, and the neutral instructions to manipulate observers' expectations about their path of travel during simulated rotation. If the instructions influence the interpretation of the retinal flow pattern in this cue conflict situation, we would expect more accurate path judgments with the straight path and the neutral instructions than with the curved path instructions across all dot conditions. If increasing the depth range or dot density of the ground plane provides useful static depth or motion parallax information, we would also expect more accurate judgments with greater density and depth.

4.1. Method

Subjects. Thirty-seven observers were paid to participate, all students or staff at Brown. One did not finish the experiment, two others made large errors in the actual rotation condition, and another two could not understand the instructions to perform the task, so they were removed from the sample. This left 32 total in the final group. Three of them were experienced subjects who participated in Experiment 1 and the rest were naïve. Again, we observed no systematic performance differences between the experienced and the naïve observers.

Displays. Displays depicted a ground plane consisting of green random dots on a black background (see Fig. 3). A red fixation point appeared on the top of a white post that was anchored to the ground, providing a reference object in the display. Two ground depths (15 and 35 m) were crossed with two dot densities (0.7 and 2 dots/m^2), generating four display conditions. (1) *15 m depth, low density:* 1050 green dots were distributed on a ground plane that extended 15 m in depth and 100 m in width from the eye point (Fig. 3a). One dot was positioned in each cell (1.43 m wide $\times$ 1 m deep) of a rectangular grid on the ground, and was randomly jittered from the center of the cell on each trial. This resulted in a dot density of 0.7 dots/m^2. Each dot consisted of a 2×2 cluster of pixels, and an anti-aliasing routine was used so that the centroid of the cluster moved smoothly over time. (2) *15 m depth, high density:* Dot density was increased to 2 dots/m^2, with a depth range of 15 m. Thus, 3000 dots were distributed on the ground, with one dot positioned in each cell (0.5 m wide $\times$ 1 m deep) of the grid (Fig. 3b). (3) *35 m depth, low density:* The

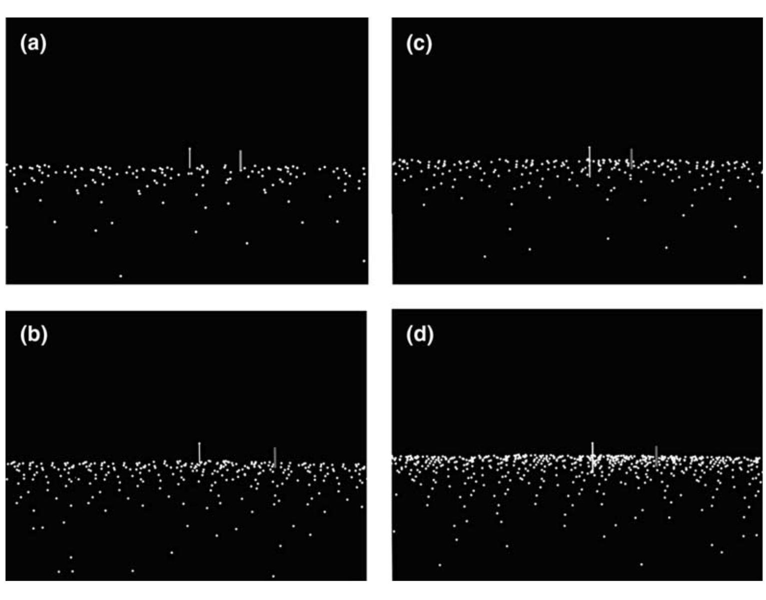

Fig. 3. A sample last frame in each display condition in Experiment 2: (a) 15 m depth low density, (b) 15 m depth high density, (c) 35 m depth low density and (d) 35 m depth high density. (The display resolution is better on the large projection screen in the experiment.)

depth range of the ground plane was increased to 35 m. 2450 dots were distributed on the ground to keep the dot density at 0.7 dots/m^2 (Fig. 3c). (4) *35 m depth, high density:* Dot density was increased to 2 dots/m^2, with a depth range of 35 m. Thus, 7000 dots were distributed on the ground (Fig. 3d).

Procedure. Trials were presented to three groups of observers. For the first group, the curved and the straight path instructions were crossed with the 15 m depth low density, the 35 m depth low density, and the 35 m depth high density displays, yielding six conditions with blocked trials. Eleven naïve and two experienced observers viewed the three types of displays in a counterbalanced order. For each display type, the testing order of the curved and the straight path instructions was also counterbalanced. The second received the neutral instructions for all the four display types, yielding four conditions with blocked trials. Nine new naïve and three experienced observers (including the two from the previous group) viewed the four types of displays in a counterbalanced order. There were 105 test trials in each testing condition, for a total of 630 trials in the first session and 420 trials in the second session. Trials were randomized within blocks, and 10 practice trials were provided before each condition commenced. As a control, the third group received the actual rotation condition with the neutral instructions for the 15 m depth low density display (42 test trials). Nine new naïve and all three experienced observers participated in the actual condition.

4.2. Results

Mean path errors for the 15 m low density, the 35 m low density, and the 35 m high density displays with the three sets of path instructions appear in Fig. 4a–c. Multivariate regression analyses show that for all the three display types, the slope for the curved path instructions is significantly larger than that for the straight path or the neutral instructions, and the straight slope is not different from the neutral slope. For the 15 m depth low density ground, the slopes are 3.56, 1.41, and 1.55 for the curved path, the straight path, and the neutral instructions respectively, and the comparisons are $t(126) = 7.26$, $p < 0.0001$, $t(184) = 6.88$, $p < 0.0001$, and $t(184) = 0.49$, *ns* (Fig. 4a); for the 35 m depth low density ground, the slopes are 2.75, 1.37, and 1.29, respectively, and the comparisons are $t(126) = 4.29$, $p < 0.0001$, $t(184) = 4.66$, $p < 0.0001$, and $t(184) = -0.27$, *ns* (Fig. 4b); and for the 35 m depth high density

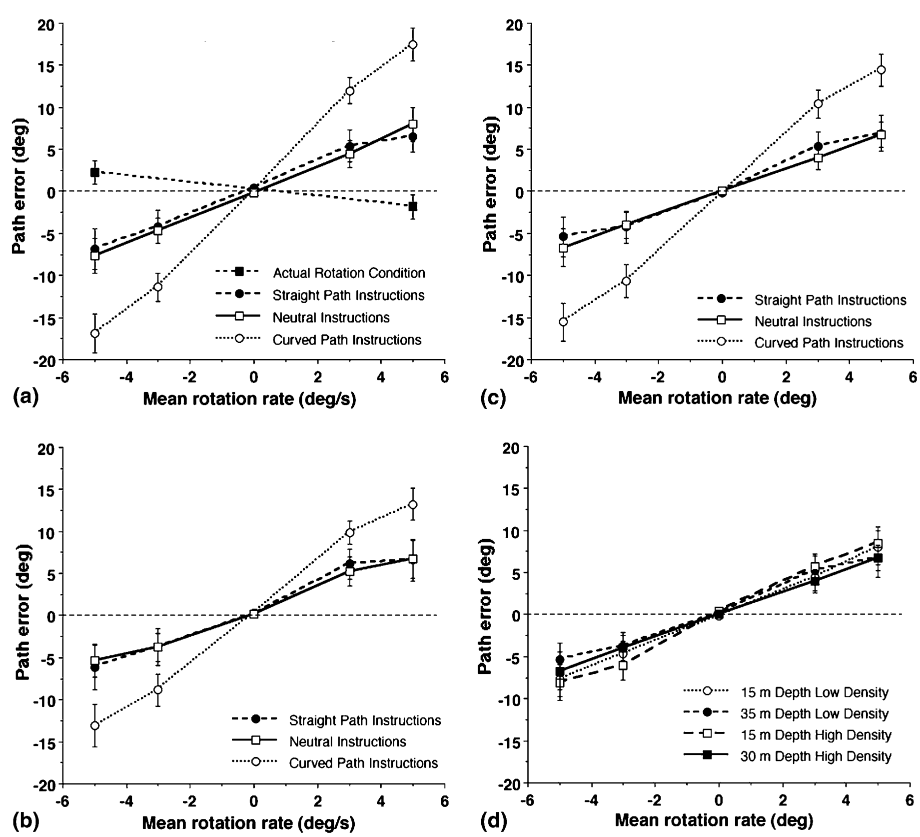

Fig. 4. Mean path error as a function of rotation rate in Experiment 2: (a) 15 m depth low density, (b) 35 m depth low density, (c) 35 m depth high density and (d) neutral instructions. Error bars represent between-subjects SEs.

ground, the slopes are 3.13, 1.33, and 1.35, respectively, and the comparisons are $t(126) = 5.98$, $p < 0.0001$, $t(184) = 6.13$, $p < 0.0001$, and $t(184) = 0.06$, *ns* (Fig. 4c). This indicates that for random-dot displays with simulated eye rotation, observers perform the same with the straight path instructions as they do with the neutral instructions, whereas the curved path instructions push observers toward a more curved interpretation of the retinal flow.

Separate analyses indicate that the slope for the straight path instructions is significantly different from 0 in all the three display conditions: for the 15 m depth low density ground, $t(126) = 6.69$, $p < 0.0001$; for the 35 m depth low density ground, $t(126) = 5.99$, $p < 0.0001$; and for the 35 m depth high density ground, $t(126) = 6.21$, $p < 0.0001$. On the other hand, the slope in the actual rotation condition for the 15 m depth low density ground (−0.40) is not statistically different from 0, $t(80) = -1.77$, ns (Fig. 4a). This pattern of results is consistent with an extra-retinal contribution to the perceived path of self-motion.

With the curved path instructions, there is a significant effect of depth range at the low dot density: the slope for the 35 m depth low density display is significantly shallower than for the 15 m depth low density display, $t(189) = -2.71$, $p < 0.01$. However, there was no such effect with the straight path instructions, $t(189) = -0.10$, *ns*. On the other hand, we observed no effect of dot density at 35 m depth range: the slope for the 35 m depth low density display is not statistically different from that for the 35 m depth high density display with either the curved path instructions, $t(189) = 1.26$, *ns*, or the straight path instructions, $t(189) = -0.14$, *ns*.

To thoroughly analyze the depth range and the dot density effects on observers' path performance, we plotted mean path errors in the four display conditions with the neutral instructions in Fig. 4d. The slope for the 35 m ground is not statistically different from that for the 15 m ground at either low or high dot density. At low dot density, the slopes for the 35 m and the 15 m ground are 1.29 and 1.55 respectively, $t(116) = 0.93$, *ns*; At high dot density, the slopes are 1.35 and 1.73, $t(116) = 1.44$, *ns*. This indicates that increasing the depth range does not improve path judgments with the neutral instructions. The increased depth range seems to reduce path errors only with the curved path instructions. Furthermore, the slope for the low density ground is not statistically different from that for the high density ground, at either 15 m depth range, $t(116) = -0.66$, *ns*, or 35 m depth range, $t(116) = -0.21$, *ns*. This confirms the findings with the straight and the curved path instructions that increasing dot density does not improve path accuracy.

Finally, we compared observers' performance on the 35 m depth high density display to that on the textured ground display in Experiment 1. With the curved path instructions, the slope is significantly higher than that for the textured ground, $t(111) = -3.34$, $p < 0.01$. With the straight path instructions, the slope is borderline higher than that for the textured ground ($t(111) = -1.89$, $p = 0.06$). With the neutral instructions, however, the slope is not significantly different from that for the textured ground, $t(106) = -0.15$, *ns*. This indicates that with the curved or the straight path instructions, observers' performance on the random-dot ground that contains the largest depth range and dot density is still not as good as that on the textured ground. With the neutral instructions, the path judgments with the random-dot ground are comparable to those with the textured ground.

4.3. Discussion

As we found in Experiment 1, the straight or curved path instructions can push observers toward the perception of a straighter or a more curved path during simulated rotation. This appears to be the case for random-dot displays with sparse structure as well as for texture-mapped displays with relatively complex structure. Nevertheless, path judgments remain significantly more accurate with texture-mapped displays, at least with the straight and curved path instructions. Furthermore, we note that path judgments with the neutral instructions are comparable to those with the straight path instructions. This suggests that retinal flow information tends to dominate with random-dot displays, even without explicit path instructions.

In the current experiment, we found that increasing the visible depth range of a random-dot ground (0.7 dots/m^2) from 15 to 35 m improved path accuracy with the curved path instructions, but not with the straight path or neutral instructions. van den Berg and Brenner (1994b) previously reported that increasing the depth range of a random-dot ground (0.5 and 0.2 dots/m^2) from 12 to 40 m reduced heading errors, consistent with a straighter perceived path of self-motion (but see Ehrlich et al., 1998). They proposed that static depth cues could help observers identify distant points near the horizon, whose motion is dominated by the rotational component of flow, allowing the visual system to estimate and remove the rotation. With a larger depth range, more distant points provide a more accurate rotation estimate, but the rotation could be attributed to either eye movement or path curvature. Thus, reduced error with the curved path instructions is somewhat paradoxical, because depth cues do not help resolve the path ambiguity. On this hypothesis, we would expect a similar effect with the straight path instructions, which we do not observe. Likewise, using the neutral instructions, we find that increasing the visible depth range does not improve path judgments. There is thus little indication that the visual system relies on distant points to estimate and remove the rotational component of flow.

One important difference between the two studies is that van den Berg and Brenner used a fixation point lying on the ground, whereas we used one on a post at eye level. Banks et al. (1996) pointed out that a fixation point on the ground plane provides a special horizon cue that observers could use to estimate heading during simulated rotation. In this case, the retinal flow pattern spirals outward from the fixation point, with a unique strip of flow vectors that are aligned in the same direction. The intersection of this strip with the horizon corresponds to the current heading point. As the depth range of the ground plane is decreased, the intersection point shifts in the direction of rotation, which could have led to increased errors with a short depth range in van den Berg and Brenner's (1994b) study. We eliminated the horizon cue by using a fixation point at eye level, and this could account for the absence of a depth range effect in the present experiment. On the other hand, it remains possible that a greater variation in the depth range (>20 m) could yield a measurable effect.

Finally, the data indicate that increasing dot density from 0.7 to 2 dots/m^2 does not improve path judgments at either 15 or 35 m depth range. We conclude that dot density does not affect the perceived path of self-motion over this density range. Theoretically, a dense motion parallax field would allow the visual system to determine the instantaneous retino-centric heading more accurately, which may be preliminary to recovering the path in the world. This finding thus seems to be at odds with our earlier proposal (Li & Warren, 2000) that path perception depends on dense motion parallax, which offered one reason why path judgments were better with dense texture-mapped displays than with sparse random-dot displays. Surprisingly, path errors were relatively small in the present experiment, remaining below 8° at 5°/s even for the 15 m low density display (neutral instructions), compared with errors up to 15° at 5°/s for Li and Warren's (2000) random-dot display (20 m depth range, 0.7 dots/m^2). With the neutral instructions, path accuracy with the random-dot ground in the present experiment is actually comparable to that with the textured ground in Experiment 1. Thus, the density of motion parallax cannot account for the improved path judgments with texture-mapped displays. We consider another explanation in Section 5.

5. General discussion

The present experiments allow us to draw several conclusions. First, we replicated previous findings that both retinal and extra-retinal information contribute to path perception during rotation (Li & Warren, 2000, 2002). In the simulated rotation condition, errors remain below 5° at a rotation rate of 5°/s with the dense posts display (neutral instructions), indicating that retinal flow is sufficient for reasonably accurate path judgments, even when in conflict with extra-retinal signals. On the other hand, accuracy improves further in the actual rotation condition, when extra-retinal signals are consistent with the retinal flow, indicating that they also contribute to path perception (Banks et al., 1996; Royden et al., 1992).

Second, we find that instructions can influence the observer's interpretation of the retinal flow pattern under the present cue conflict conditions. This is the case for both texture-mapped and random-dot displays. We suggest that straight or curved path instructions lead the visual system to differentially rely upon retinal information for object-relative heading, which specifies a straight path, or upon extra-retinal signals for zero eye rotation, which indicates a curved path. This would explain why participants believe that they have actually viewed two different classes of displays corresponding to straight and curved paths of self-motion.

Finally, the results indicate that increasing the dot density or depth range of a random-dot ground does not improve path judgments during simulated rotation, at least over the ranges tested. Surprisingly, even a low dot density of 0.7 dots/m^2 and the shorter depth range of 15 m yielded relatively accurate path judgments, with errors below 8° at high rotation rates. This indicates that denser motion parallax is unlikely to account for the improved performance with texture-mapped displays reported by Li and Warren (2000). With the dense posts display, there is a similarly low density of motion parallax between posts (0.5 posts/m^2), yet path judgments are the most accurate. A relatively low density of motion parallax thus appears to be sufficient for a reasonably accurate path perception. In addition, we found no evidence that a more distant horizon (35 m vs. 15 m) contributes to compensating for rotation with either the straight path or the neutral instructions.

The remaining puzzle is the unexpectedly good performance we observed for random-dot displays with the neutral instructions, which had an accuracy comparable to that for the textured ground display. Path error in Experiment 2 remained below 8° at 5°/s, half of Li and Warren's (2000) error of 15° at 5°/s with a random-dot ground. We believe that the improved accuracy in the present study can be attributed to a larger field of view. The present random-dot displays, as well as Li and Warren's (2000) texture-mapped displays, subtended a large visual angle (112° H × 95° V), whereas the random-dot display of Li and Warren (2000) and previous researchers (Banks et al., 1996; Ehrlich et al., 1998), had a field of view less than two-thirds this size (69° H × 59° V). As shown formally by Koenderink and van Doorn (1987), a large field of view improves the estimation of rotation from the retinal flow and increases the magnitude of motion parallax in the peripheral regions of the display. Consistent with this observation, Grigo and Lappe (1999) reported accurate heading judgments with a large frontal plane of dots (90° H × 90° V), whereas previous researchers had found high errors for small displays of a frontal plane (40° H × 32° V, Warren & Hannon, 1990). In the present case, a larger field of view may have allowed the visual system to determine the instantaneous heading more accurately, even at low dot densities. In combination with a reference object (the fixation post), this may have permitted better object-relative path judgments.

In sum, the present results are consistent with Li and Warren (2000, 2002) (Warren, 2004) proposal that one's path through the environment can be determined from retinal flow. Specifically, we argue that the instantaneous retino-centric heading is determined from motion parallax between elements at different depths, which is particularly effective over a large field of view. The rotational component is simultaneously determined by detecting the lamellar flow over a large field of view. The path through the world is then recovered by updating the heading with respect to objects in the scene over time. Recent evidence suggests that extra-retinal signals may merely serve to indicate whether or not the eye is rotating (Crowell & Andersen, 2001), thereby gating the interpretation of the lamellar flow as being due to eye rotation or to a curved path of self-motion. During simulated rotation, extra-retinal signals conflict with the retinal flow and reference objects. In this case the latter tend to dominate, with a partial extra-retinal influence, leading to perception of the object-relative path with slight curvature in the direction of rotation. This is supported by our finding that performance with the neutral instructions is closer to that with the straight path than with the curved path instructions, and in some cases the two are not significantly different. With more objects in the scene, as in the dense posts display, the visual frame of reference they provide is more strongly defined and the object-relative path is determined more accurately.

Acknowledgements

This research was supported by grants from the National Institutes of Health, EY10923 and K02 MH01353. We thank Lee Stone for helpful discussions, and Tram Nguyen and Lindsay Mann for their assistance.

References

Banks, M. S., Ehrlich, S. M., Backus, B. T., & Crowell, J. A. (1996). Estimating heading during real and simulated eye movements. *Vision Research, 36*, 431–443.

Crowell, J. A., & Andersen, R. A. (2001). Pursuit compensation during self-motion. *Perception, 30*, 1465–1488.

Cutting, J. E., Springer, K., Braren, P. A., & Johnson, S. H. (1992). Wayfinding on foot from information in retinal, not optical, flow. *Journal of Experimental Psychology: General, 121*, 41–72.

Cutting, J. E., Vishton, P. M., Fluckiger, M., Baumberger, B., & Gerndt, J. D. (1997). Heading and path information from retinal flow in naturalistic environment. *Perception and Psychophysics, 59*, 426–441.

Ehrlich, S. M., Beck, D. M., Crowell, J. A., Freeman, T. C. A., & Banks, M. S. (1998). Depth information and perceived self-motion during simulated gaze rotations. *Vision Research, 38*, 3129–3145.

Gibson, J. J. (1950). *Perception of the visual world*. Boston: Houghton Mifflin.

Grigo, A., & Lappe, M. (1999). Dynamical use of different sources of information in heading judgments from retinal flow. *Journal of the Optical Society of America A, 16*, 2079–2091.

Koenderink, J. J., & van Doorn, A. J. (1987). Facts on optic flow. *Biological Cybernetics, 56*, 247–254.

Li, L., Peli, E., & Warren, W. H. (2002). Heading perception in patients with advanced retinitis pigmentosa. *Optometry and Vision Science, 79*(9), 581–589.

Li, L., & Warren, W. H. (2000). Heading perception during rotation: Sufficiency of dense motion parallax and reference objects. *Vision Research, 40*, 3873–3894.

Li, L., & Warren, W. H. (2002). Retinal flow is sufficient for steering during observer rotation. *Psychological Science, 13*(5), 485–491.

Perrone, J. A. (1992). Model for the computation of self-motion in biological systems. *Journal of the Optical Society of America A, 9*, 177–194.

Rieger, J. H., & Lawton, D. T. (1985). Processing differential image motion. *Journal of the Optical Society of America A, 2*, 354–360.

Royden, C. S. (1994). Analysis of misperceived observer motion during simulated eye rotations. *Vision Research, 34*, 3215–3222.

Royden, C. S., Banks, M. S., & Crowell, J. A. (1992). The perception of heading during eye movements. *Nature, 360*, 583–585.

Royden, C. S., Crowell, J. A., & Banks, M. S. (1994). Estimating heading during eye movements. *Vision Research, 34*, 3197–3214.

Stone, L. S., & Perrone, J. A. (1997). Human heading estimation during visually simulated curvilinear motion. *Vision Research, 37*, 573–590.

van den Berg, A. V. (1992). Robustness of perception of heading from optic flow. *Vision Research, 32*(7), 1285–1296.

van den Berg, A. V., & Brenner, E. (1994a). Why two eyes are better than one for judgments of heading. *Nature, 371*, 700–702.

van den Berg, A. V., & Brenner, E. (1994b). Humans combine the optic flow with static depth cues for robust perception of heading. *Vision Research, 34*, 2153–2167.

Wang, R. F., & Cutting, J. E. (1999). Where we go with a little good information. *Psychological Science, 10*, 72–76.

Warren, W. H. (2004). Optic flow. In L. Chalupa & J. Werner (Eds.), *The visual neurosciences* (pp. 1247–1259). Cambridge, MA: MIT press.

Warren, W. H., Blackwell, A. W., Kurtz, K. J., Hatsopolous, N. G., & Kalish, M. (1991). On the sufficiency of the velocity field for perception of heading. *Biological Cybernetics, 65*, 311–320.

Warren, W. H., & Hannon, D. J. (1988). Direction of self-motion is perceived from optical flow. *Nature, 336*, 162–163.

Warren, W. H., & Hannon, D. J. (1990). Eye movements and optical flow. *Journal of the Optical Society of America A, 7*(1), 160–169.

Warren, W. H., Kay, B. A., Zosh, W. D., Duchon, A. P., & Sahuc, S. (2001). Optic flow is used to control human walking. *Nature Neuroscience, 4*, 213–216.

Warren, W. H., Morris, M. W., & Kalish, M. (1988). Perception of translation heading from optical flow. *Journal of Experimental Psychology: Human Perception and Performance, 14*, 646–660.